Electronic Supplementary Material (ESI) for Dalton Transactions

SUPPORTING INFORMATION

MgO-Supported Bimetallic Catalysts Consisting of Segregated, Essentially Molecular Rhodium and Osmium Species

Joseph D. Kistler, [a] **Pedro Serna**[a] **and Bruce C. Gates***[a]

Table S1. Table of Assignment of infrared bands in the ν_{CO} region of initial samples on MgO prepared from (a) $Os_3(CO)_{12}$ (b) $Rh(C_2H_4)_2(acac)$ followed by a CO pulse and (c) $Os_3(CO)_{12}$ and $Rh(C_2H_4)_2(acac)$ adsorbed in that order

(a) $[Os_3(CO)_{11}]^{2-}$	(b) $Rh(CO)_2$	(c)$[Os_3(CO)_{11}]^{2-}$ + $Rh(C_2H_4)_2$	Assignment
2079		2080	(C≡O)terminal[16]
	2075		C≡O Stretching
2010		2010	(C≡O)terminal [16]
	1995		C≡O Stretching
1935		1930	(C≡O)terminal [16]

Table S2. Table of Assignment of Infrared Bands in the ν_{CH} region of initial samples on MgO prepared from (d) $Rh(C_2H_4)_2(acac)$ and (e) $Os_3(CO)_{12}$ and $Rh(C_2H_4)_2(acac)$ adsorbed in that order

(d)$Rh(C_2H_4)_2$	(e)$[Os_3(CO)_{11}]^{2-}$ + $Rh(C_2H_4)_2$	Assignment
3080	3080	(C_3-H)(acac) [3]
3064	3060	(CH_2)(ethylene) [3]
2996	3001	(CH_3)(acac) [3]
2964	2960	(CH_3)(acac) [3]
2927	2931	(CH_3)(acac) [3]
2851	2853	Combination band[3]

Table S3. Table of Assignment of Infrared Bands in the ν_{CO} region of samples from Table S1 after treatment at 393 K in H_2 and a pulse of CO

(a)$[Os_3(CO)_{11}]^{2-}$	(b)$Rh(CO)_2$	(c)$[Os_3(CO)_{11}]^{2-}$ + $Rh(C_2H_4)_2$	Assignment
2090			Terminal Carbonyls
	2072	2080	Terminal Carbonyls
	2047		Terminal Carbonyls
2030			Terminal Carbonyls
2015		2010	Terminal Carbonyls
	2005		Terminal Carbonyls
1990			
1935		1933	Bridging Carbonyls
	1890		Bridging Carbonyls

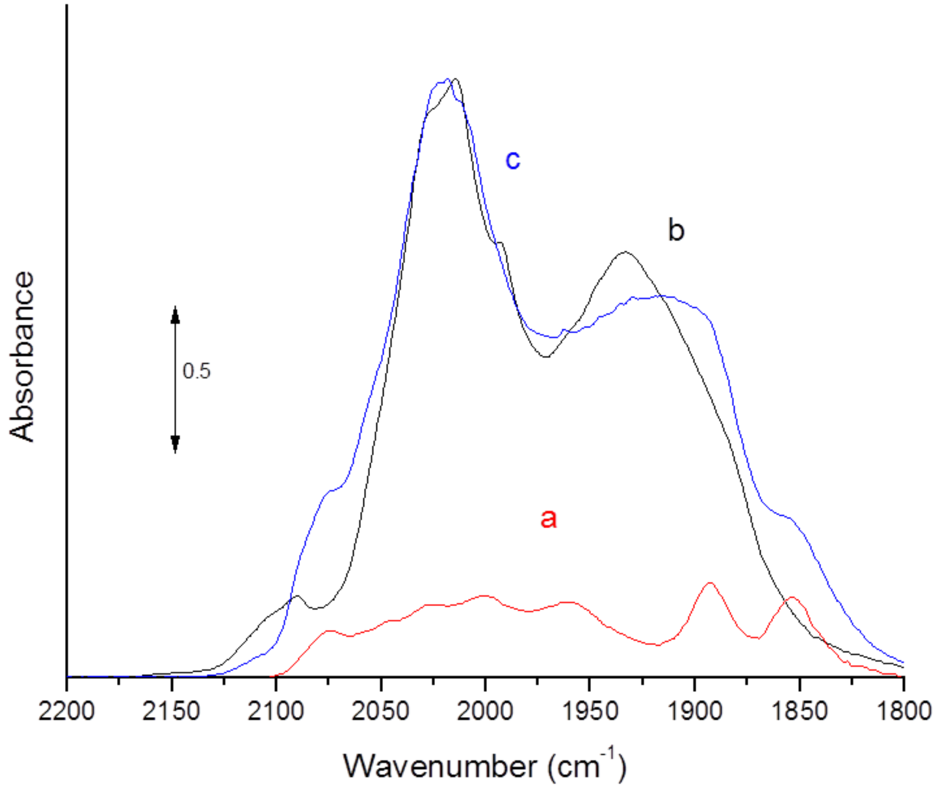

Figure S1. IR spectra (absorbance) in the ν_{CO} region characterizing MgO-supported samples treated at 393 K for 1 h in flowing H_2 followed by a CO pulse at 298 K: (a) $Rh(C_2H_4)_2$, (b) $[Os_3(CO)_{11}]^{2-}$, (c) $[Os_3(CO)_{11}]^{2-}$ + $Rh(C_2H_4)_2$.

Table S4. EXAFS fit parameters characterizing supported osmium and rhodium species at the Os L3 edge and the Rh K edge: (1) Sample 1, formed from adsorption of $Rh(C_2H_4)_2(acac)$ on MgO (Δk = 3.8–13.3 Å^{-1}, ΔR = 0.8–4.0 Å); (2) Sample 2, which is Sample 1 after treatment with continuously flowing H_2 at 353 K for 1 h (Δk = 3.1–13.9 Å^{-1}, ΔR = 0.8–4.0 Å); (3) Sample 3, formed from adsorption of $Os_3(CO)_{12}$ on MgO (Δk = 2.7–12.3 Å^{-1}, ΔR = 0.8–4.0 Å); (4) Sample 4, which is Sample 3 after treatment with continuously flowing H_2 at 393 K for 1 h (Δk = 3.46–12.53Å^{-1}, ΔR = 0.8–4.0 Å); (5) Sample 5, formed from adsorption of $Os_3(CO)_{12}$ followed by $Rh(C_2H_4)_2(acac)$ on MgO taken at the Os L3 edge (Δk = 3.1–12.9 Å^{-1}, Δr = 0.8–4.0 Å); (6) Sample 6, which is the same as sample 5 but with data taken at the Rh K edge (Δk = 2.8–13.0 Å^{-1}, ΔR = 0.8–4.0 Å); (7) Sample 7, which is Sample 5 after treatment with continuously flowing H_2 at 393 K for 1 h taken at the Os L3 edge (Δk = 2.7–11.6 Å^{-1}, Δr = 0.8–4.0 Å); (8) Sample 8, which is the same as sample 5 but with data taken at the Rh K edge (Δk = 3.3–11.7 Å^{-1}, Δr = 0.8–4.0 Å);

Sample	Shell	N	R (Å)	10^3 x $\Delta\sigma^2$ (Å^2)	ΔE_0 (eV)	ref
1	Rh-Rh	-	-	-	-	3
$Rh(C_2H_4)_2$/MgO	Rh–$C_{ethylene}$	4.0	2.04	0.68	6.20	
	Rh–$O_{support}$	1.8	2.18	0.86	-6.13	
	Rh–Mg	1.83	3.09	8.80	-2.45	
2	Rh–Rh	1.0	2.71	5.8	-2.9	4
$Rh(C_2H_4)_2$/MgO	Rh–C_{ethyl}	1.2	2.09	0.01	6.9	
	Rh–$O_{support}$	1.0	2.21	2.7	7.2	
	Rh–Mg	0.7	2.86	0.07	0.6	
3	Os–Os	2.2	2.89	3.30	2.31	5
$[Os_3(CO)_{11}]^{2-}$/MgO	Os–C_{CO}	3.2	1.89	3.45	6.61	
	Os–O_{CO}	3.2	3.03	3.92	4.68	
	Os–$O_{support}$	0.9	2.12	-1.54	-4.59	
4	Os–Os	2.1	2.84	1.44	5.50	This work
$[Os_3(CO)_{11}]^{2-}$/MgO	Os–C_{CO}	1.86	1.87	2.22	3.24	
	Os–O_{CO}	1.86	2.95	2.86	7.54	
	Os–$O_{support}$	0.9	2.08	0.05	-6.22	
5	Os–Os	1.96	2.78	10.75	-5.55	This work

$[Os_3(CO)_{11}]^{2-}$ + $Rh(C_2H_4)_2$/MgO	Os–Rh	-	-	-	-	
	Os–C_{CO}	1.76	1.96	4.88	1.83	
	Os–O_{CO}	1.76	3.04	5.36	-5.76	
	Os–$O_{Support}$	0.9	2.08	-0.1	-1.62	
6	Rh–Rh	--	--	--	--	This work
$[Os_3(CO)_{11}]^{2-}$ + $Rh(C_2H_4)_2$/MgO	Rh–Os	--	--	--	--	
	Rh–$C_{ethylene}$	4.02	2.07	0.87	-1.00	
	Rh–$O_{support}$	2.16	2.14	1.42	1.15	
	Rh–Mg	0.99	2.946	0.50	-3.77	
7	Os–Os	1.9	2.65	1.8	6.31	This work
$[Os_3(CO)_{11}]^{2-}$ + $Rh(C_2H_4)_2$/MgO	Os–Rh	-	-	-	-	
	Os–C_{CO}	1.5	1.97	0.88	1.21	
	Os–O_{CO}	1.5	3.13	2.99	3.68	
	Os–$O_{Support}$	0.9	0.55	2.01	-7.04	

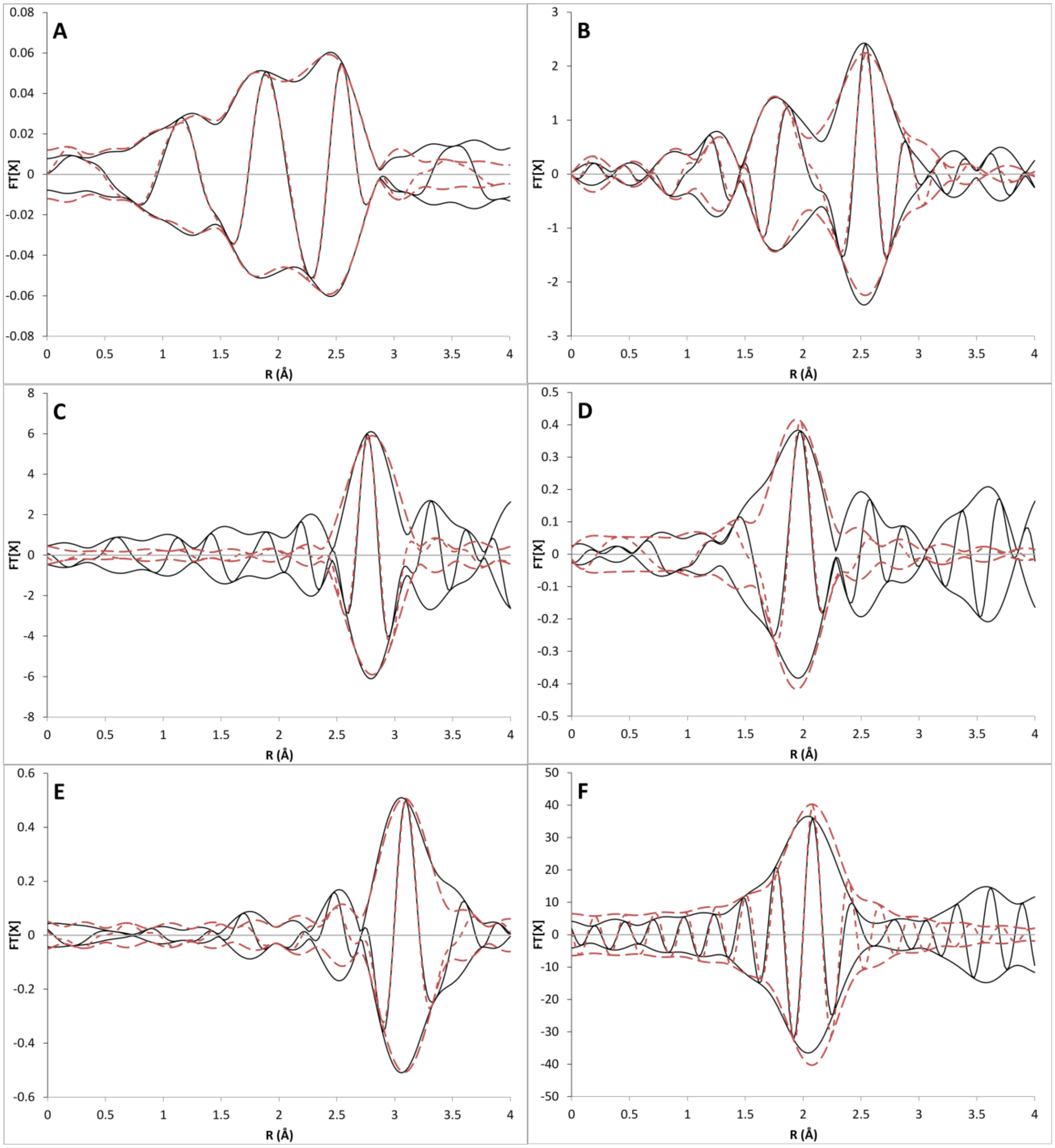

Figure S2. EXAFS data characterizing initially prepared MgO-supported $[Os_3(CO)_{11}]^{2-}$ and $Rh(C_2H_4)_2$; the spectra were recorded as the sample was in helium flowing at 298K: (A) k^1-weighted EXAFS data (solid line) and the best fit (dashed line). (B) Magnitude and imaginary part of Fourier transform of k^3-weighted EXAFS data (solid line) and the best fit (dashed line) (C) k^3-weighted, phase-corrected, imaginary part and magnitude of the Fourier transform of the data (solid line) and calculate contributions (dashed line) of Os-Os shell; EXAFS data (solid line) and the best fit (dashed line); (D) k^1-weighted, phase-corrected, imaginary part and magnitude of the Fourier transform of the data (solid line) and calculate contributions (dashed line) of Os-$C_{carbonyl}$ shell; EXAFS data (solid line) and the best fit (dashed line); (E) k^1-weighted, phase-corrected, imaginary part and magnitude of the Fourier transform of the data (solid line) and calculate contributions (dashed line) of Os-$O_{carbonyl}$ shell; EXAFS data (solid line) and the best fit (dashed line); (F) k^3-weighted, phase-corrected, imaginary part and magnitude of the Fourier transform of the data (solid line) and calculate contributions (dashed line) of Os-$O_{support}$ shell; EXAFS data (solid line) and the best fit (dashed line);

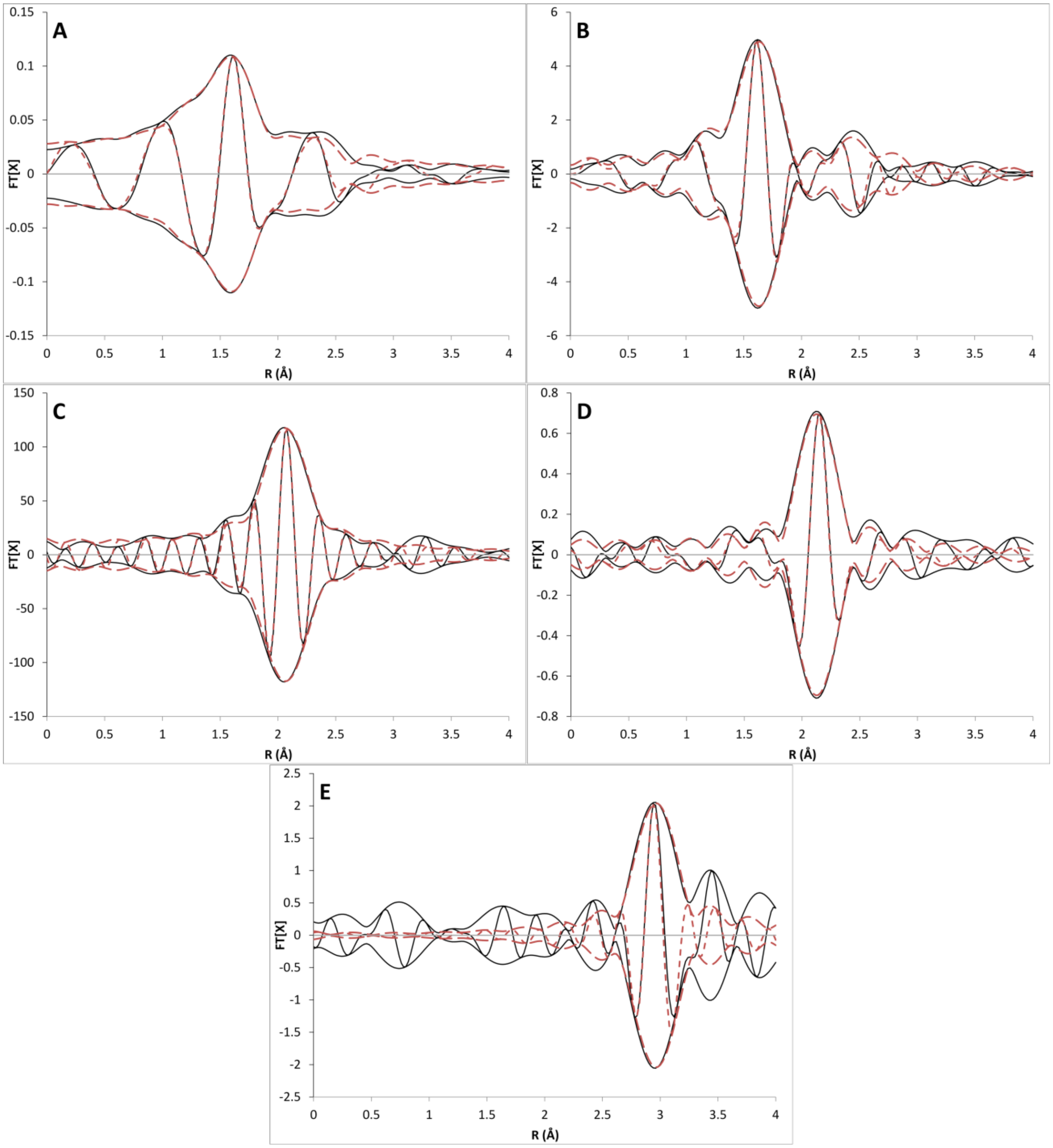

Figure S3. EXAFS data characterizing initially prepared MgO-supported $[Os_3(CO)_{11}]^{2-}$ and $Rh(C_2H_4)_2$; the spectra were recorded as the sample was in helium flowing at 298 K: (A) Magnitude and imaginary part of Fourier transform of k^1-weighted EXAFS data (solid line) and best fit of the data (dashed line); (B) k^3-weighted, phase-corrected, imaginary part and magnitude of the Fourier transform of the data (solid line) and calculated contributions (dashed line) of Rh–$C_{ethylene}$ shell; EXAFS data (solid line) and best fit of the data (dashed line); (C) k^1-weighted, phase-corrected, imaginary part and magnitude of the Fourier transform of the data (solid line) and calculated contributions (dashed line) of Rh–$C_{ethylene}$ shell; EXAFS data (solid line) and best fit of the data (dashed line); (D) k^1-weighted, phase-corrected, imaginary part and magnitude of the Fourier transform of the data (solid line) and calculated contributions (dashed line) of Rh–$O_{support}$ shell; EXAFS data (solid line) and best fit of the data (dashed line); (E) k^3-weighted, phase-corrected, imaginary part and magnitude of the Fourier transform of the data (solid line) and calculated contributions (dashed line) of Rh–Mg shell; EXAFS data (solid line) and best fit of the data (dashed line).